STABILITY PERFORMANCE OF SUSPENSION BRIDGES WITH A RECTANGULAR, A TRAPEZOIDAL AND A HEXAGONAL CROSS-SECTIONS

Fuh-Min Fang[*], Yi-Chao Li[†1], and Chu-Chang Chen[†2]

[*]Department of Civil Engineering
National Chung Hsing University, 250 Kuo Kuang Road, Taichung, Taiwan
e-mail: fmfang@nchu.edu.tw

[†1]Architecture and Building Research Insititute
Ministry of the Interior, 200, Section 3, Beisin Road, Sindian, Taipei County, Taiwan
e-mails: scottlee@abri.gov.tw

[†2]Department of Information Management
Chung Chou Institute of Technology, 6, Lane 2, Shan-Cjiao Road, Changhwa, Taiwan
e-mail: bljcchen@dragon.ccut.edu.tw

Keywords: Fluid-structure Interaction, Section Model, Numerical Simulation.

ABSTRACT

The aerodynamic instability of suspension bridges with a rectangular, a trapezoidal and a hexagonal cross-sections respectively were investigated based on the concept of a section model. Measurements of the root-mean-square responses in the vertical and torsional directions of three bridge models at various wind speeds were conducted firstly in a wind tunnel and the results were obtained to confirm those from the parallel numerical simulations. After the validity of the numerical method was verified, both the experimental and numerical results were used to examine the flow effect as well as the aeroelastic behavior of the bridges in detail, and further to assess and compare the stability performance of the bridges with the three different shapes.

Results show that the predictions of the root-mean-square bridge responses agree well with those from the section model measurements, indicating that the present numerical method can be used to analyze the problem with good accuracy. In addition, based on the numerical results in time series, the variations of net damping ratios and flutter derivatives associated with the three bridge decks are analyzed extensively. Finally, it is found that the rectangular deck leads to the least flutter speed or the worst aerodynamic instability among all the cases. On the other hand, the hexagonal deck, with an increase of about 17% in terms of the critical flutter speed, possesses the best stability performance.

1   INTRODUCTION

The aerodynamic instability of a suspension bridge is generally a major concern in design since the long-span structure is sensitive to wind. Physically, when wind passes the bridge, which usually possesses a blunt shape, vortex shedding occurs and leads to unsteady wind load on the structure. If the extent of the resulting bridge vibration is significant, it can affect the surrounding flow and further promote the structural response. Therefore, the analysis of the interaction between the structure motion and the wind flow is considered necessary.
Besides the physical properties of the bridge, the shape of the bridge deck is also an important factor in affecting its aerodynamic behavior. To investigate the effect of the deck shape, three basic geometries of the deck cross-sections (a rectangle, a trapezoid and a hexagon) are selected for the analyses based on the concept of a section model. By performing extensive examinations on the resulting fluctuating responses, net damping ratios and flutter derivatives, the instability associated with the three bridge decks are assessed. Finally, the aerodynamic performances of the three bridge decks are compared in terms of the critical flutter speeds.

2   PROBLEM DESCRIPTIONS

Wind tunnel tests and numerical simulations are used to analyze the dynamic behavior of the three bridge decks. The geometries of the corresponding section models are shown in Fig. (1). The thicknesses of the decks (D) are 4 cm. For better comparison, the widths of the upper surfaces of all the decks (B′) are the same (B = 8D = 32 cm). The side angles of the trapezoidal and hexagonal decks are chosen typically as 60°. Table 1 illustrates the related physical quantities of the sectional deck models.
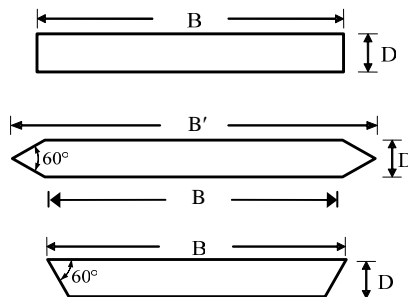

Figure 1: Geometries of the three deck cross-sections.

Shape	Mass (M) (kg/m)	Momentum of inertia (I) (kg-m²/m)	Fundamental frequency (Hz)			Damping ratio (%)	
			Vertical (f_V)	Torsional (f_T)	Frequency ratio (f_T/f_V)	Vertical (ξ_V)	Torsional (ξ_T)
Rectangle	3.785	1.29×10^{-2}	9.86	20.53	2.08	0.54	0.77
Trapezoid	3.634	1.10×10^{-2}	9.93	20.69	2.08	0.56	0.78
Hexagon	3.861	1.31×10^{-2}	9.74	20.62	2.12	0.58	0.72

Table 1: Related physical properties of the sectional deck models.

Fig. (2) depicts the schematic of the problem. The mass distributions of the bridge cross-sections are assumed uniform so that the effect due to eccentricity is not of concern. At five selected attack angles ($\beta = 0°$, $\pm 4°$ and $\pm 8°$), the approaching flow is considered smooth with a speed (U) varying from 2 to about 48 m/s in the numerical predictions and 2 to about 20 m/s in the model experiments.
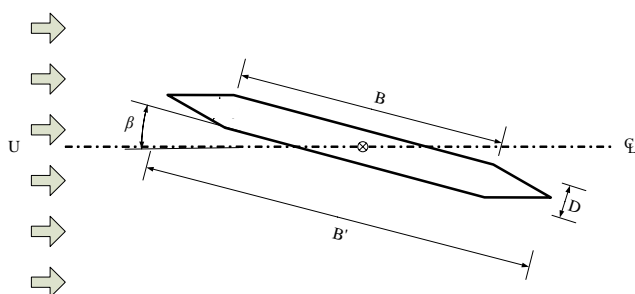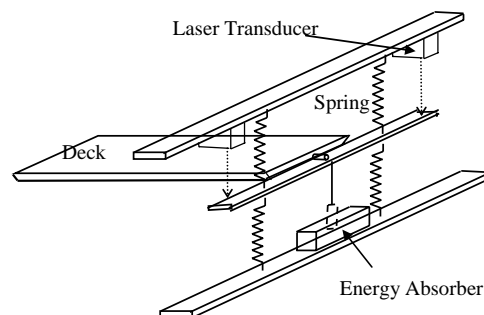
Figure 2: Sketch of problem.

Figure 3: Setup of section model experiments.

3 EXPERIMENTAL PROGRAM AND NUMERICAL METHOD

In the model experiments, the decks are installed on a suspended rack mechanism, (see Fig. (3)) in a 80 cm $\times$ 80 cm test section with a blockage ratio less than 5%. An energy absorber, filled with a viscous liquid, is set to produce appropriate damping in the vertical and torsional directions. Hot-film anemometry is used to measure the approaching flow speed. Four laser transducers are set on the rack mechanism to monitor the motion of the vibrating model decks.

The numerical simulations contain two separate computations which are performed by an interactive procedure. To predict the unsteady flow around the decks, a weakly-compressible-flow method [1] with a dynamic subgrid-scale turbulence model [2] is applied. After an instantaneous flow field is simulated, the resulting wind load is taken as an input to further compute the corresponding structure responses. The resulting deflections and the vibrating speeds of the deck are then fed back to the boundary specifications at the deck surfaces for the flow calculations in the next time step. The alternative solutions of the flow field and the deck motion are considered the results of the interactive dynamic behavior of the two.

4 RESULTS

Figs. (4) and (5) show the resulting root-mean-square values of the vertical and torsional deck deflections at various reduced velocities, defined as $Ur = U/(f_V B)$. It can be seen that good agreements between the sets of measurement results and numerical predictions are obtained. Generally, the root-mean-square deflections in both the across-wind and torsional directions increase as the reduced velocity increases, except when two resonances occur, leading to the occurrence of local peak values. When Ur reaches about 13.41, 14.32 and 15.80 respectively, the root-mean-square responses in both the directions become diverged.

Based on the numerical results, Figs. (6) and (7) show the variations of the net damping ratios. In general, the variation of the ratio in the across-wind direction starts with the value of the material damping then increase monotonically with an increase of the wind speed. In the torsional direction, in contrast, the variation pattern of the net damping ratios appears entirely different. It starts with the material damping value and increases with an increase in the wind speed. After reaching a peak value, the ratio then decreases. Finally, it drops to a zero value at the same instants as those of the onsets of response divergences. Accordingly, one can conclude that although the fluctuating responses diverge in both directions at these critical speeds, the instability of all the decks is actually subject to torsional flutter.

As the onset of flutter is initiated when the net damping ratio becomes zero, the critical flutter speed can be accurately evaluated based on the numerical results from Fig. (7). Among the three cases, accordingly, the rectangular deck possesses the worst stability performance and the best is the hexagonal deck, whose critical flutter speed is about 17% greater than that of the rectangular deck.
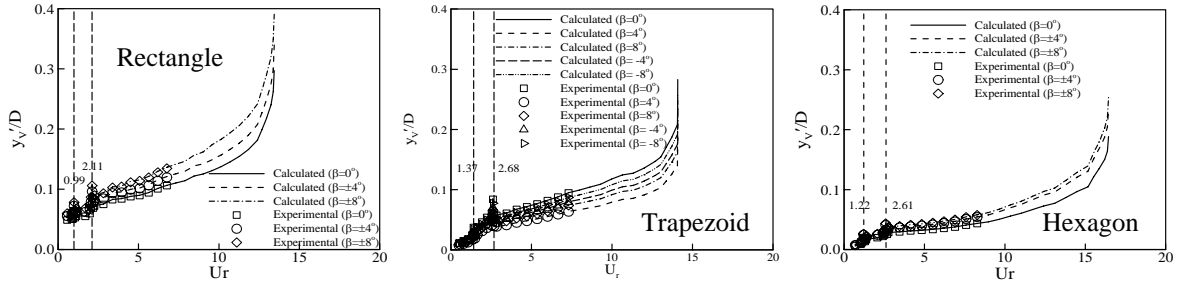
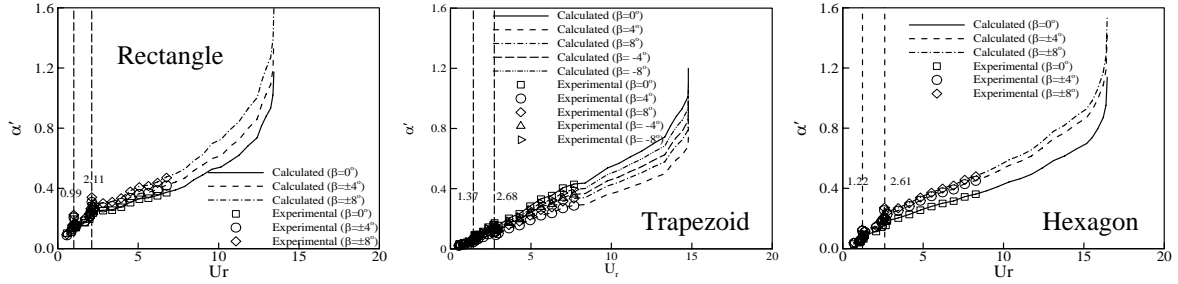Figure 4: Root-mean-square vertical responses of the decks.

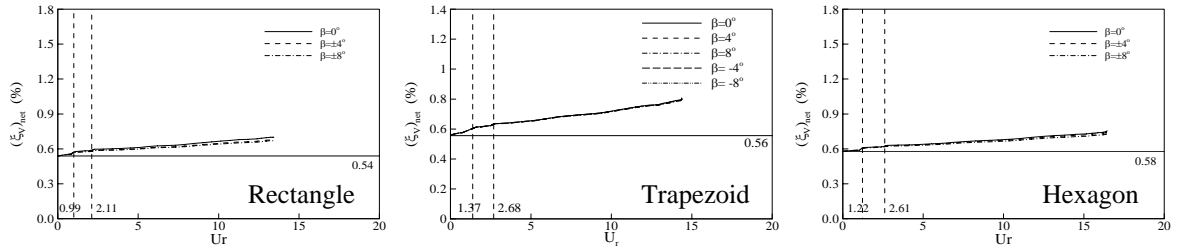Figure 5: Root-mean-square torsional responses of the decks.

Figure 6: Calculated net damping ratios in the vertical direction.
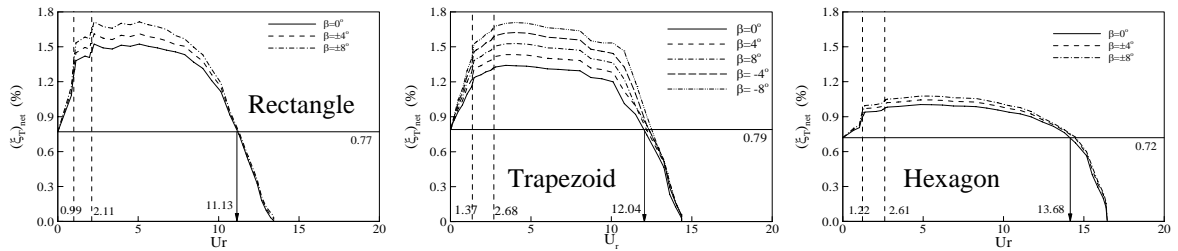

Figure 7: Calculated net damping ratios in the torsional direction.

ACKNOWLEDGEMENTS

REFERENCES

[1] C.C.S. Song and M. Yuan, A weakly compressible flow model and rapid convergence methods. *Journal of Fluids Engineering*, **110**, 441-455, 1988.

[2] M. Germano, U. Piomelli, P. Moin and W.H. Cabot, A dynamic subgrid-scale eddy viscosity model. *Physics of Fluids*, **3**, 1760-1765, 1991.